



# Selection of stimulated Raman scattering signal by entangled photons



Purevdorj Munkhbaatar<sup>a,b</sup>, Kim Myung-Whun<sup>b,c,\*</sup>

<sup>a</sup> Department of Physics and Electronics, National University of Mongolia, Ulaanbaatar 210646, Mongolia

<sup>b</sup> Institute of Photonics and Information Technology, Chonbuk National University, Jeon-ju 54896, Republic of Korea

<sup>c</sup> Department of Physics, Chonbuk National University, Jeon-ju 54896, Republic of Korea

## ARTICLE INFO

### Keywords:

Excitation-probe measurement

Entangled photon pulses

Stimulated Raman scattering

## ABSTRACT

We propose an excitation-probe measurement method utilizing entangled photon pulses. The excitation-probe signal is dominated by stimulated Raman scattering as well as two-photon absorption when the time delay between the excitation pulse and the probe pulse is shorter than the pulse duration. We demonstrate that the two-photon-absorption signal can be suppressed when the photons of the pulses are entangled. The stimulated Raman scattering signal can be composed of many peaks distributed over broad photon energies owing to the transitions between numerous quantum states in complex materials. We show that the desired peaks among the many peaks can be selected by controlling the thickness of the nonlinear crystal, the pump pulse center frequency, and the polarization of the excitation pulse and probe pulse.

## 1. Introduction

Excitation-probe (or pump-probe) technique is useful to investigate the optical excitations between quantum states of matter [1,2]. Light pulse can excite electric charges, thereby creating an excited state in the sample material. The excited state decays spontaneously to the ground state or to a quasi-ground state by emitting photon fields. In the presence of strong radiation such as in the excitation-probe measurement, stimulated emission becomes more dominant while spontaneous emission becomes negligible. During the excitation-probe measurement, a part of probe pulse interferes with the emitted photon field, producing measurable change in the intensity of probe pulse itself, which often appears as sinusoidal function of pulse delay time [3]. The sinusoidal modulation is the signature of a stimulated Raman scattering (SRS) process in the sample material [4–6].

In complex materials, various interactions participate in the formation of Raman active modes. Simple harmonic lattice interaction is most prevailing, but spin-exchange or orbital-exchange interaction between neighboring charges also constitute Raman active modes [1]. The interactions are often strongly coupled to each other, so independent modes can be merged into one composite mode soon after the excitation. Early time-delay signal of the excitation-probe measurement is essential to understand the intrinsic properties of the Raman modes. However, the conventional excitation-probe signal suffers from the strong nonlinear background when excitation pulse and probe pulse are overlapped. Fortunately, stimulated Raman scattering (SRS) and two-photon absorption (TPA) are dominant in simple excitation-

probe processes [3]. If it is possible to separate the TPA signal from the SRS signal in typical excitation-probe measurement geometry, the early time-delay SRS signal can be investigated by the excitation-probe measurement.

Some techniques have been invented to discriminate the SRS and TPA signals. Some of the techniques utilized the combinations of classical optical devices including electro-optical or acousto-optical devices [7,8]. Recently, quantum mechanically entangled light becomes used to improve the performance of nonlinear spectroscopic techniques. A theoretical approach showed that the intensity of TPA can be manipulated in the excitation-probe measurement if entangled photons were used [9]. A quantum SRS technique was proposed theoretically, which suggested the combination of entangled light source produced via type-II parametric down conversion and Hanbury–Brown–Twiss type interferometry to enhance the resolution and selectivity of Raman signals [10]. The study theoretically demonstrated that SRS signals obtained by the sixth-order perturbation of entangled photon pulse fields can eliminate the off-resonant background and can select Raman gain and Raman loss processes. However, so far it has been rarely shown the way to suppress the intensity of TPA in the excitation-probe measurement by utilizing the entanglement of photon pulse excitation-probe measurement.

Conventional excitation-probe measurements in many laboratories are performed with two optical modes with wave vectors  $k_1$  and  $k_2$  and frequencies  $\omega_1$  and  $\omega_2$  in the simplest description. We have thought about a way of suppressing TPA signal in two-mode geometry. Suppose  $(k_1, \omega_1)$  is the excitation mode and  $(k_2, \omega_2)$  is the probe mode. Typical

\* Corresponding author at: Institute of Photonics and Information Technology, Chonbuk National University, Jeon-ju 54896, Republic of Korea.  
E-mail address: [mwkim@chonbuk.ac.kr](mailto:mwkim@chonbuk.ac.kr) (K. Myung-Whun).

measurement detects the intensity change of the  $(k_2, \omega_2)$  mode resulting from the cooperation of the eight quantum pathways invoked by the  $(k_1, \omega_1)$  mode. The pathways are divided into the TPA group and the SRS group [9]. All the pathways in the TPA group contain optical correlation functions of the form  $\langle a^\dagger a^\dagger aa \rangle$ ; here,  $a(a^\dagger)$  is the annihilation (creation) operator of the optical modes. The possible optical correlation functions for the TPA pathways are  $\langle a_2^\dagger a_1^\dagger a_1 a_2 \rangle$ ,  $\langle a_2^\dagger a_1^\dagger a_2 a_1 \rangle$ ,  $\langle a_1^\dagger a_2^\dagger a_2 a_1 \rangle$ , and  $\langle a_1^\dagger a_2^\dagger a_1 a_2 \rangle$ . The optical correlation functions of the SRS group are  $\langle a_2^\dagger a_2 a_1^\dagger a_1 \rangle$ ,  $\langle a_2^\dagger a_1 a_1^\dagger a_2 \rangle$ ,  $\langle a_1^\dagger a_1 a_2^\dagger a_2 \rangle$ , and  $\langle a_1^\dagger a_2 a_2^\dagger a_1 \rangle$ . For the classical optical modes, the intensity change due to all of the eight correlation functions become identical:  $\langle a_2^\dagger \rangle \langle a_1^\dagger \rangle \langle a_2 \rangle \langle a_1 \rangle \sim |E_1|^2 |E_2|^2$  [9,11]. This is the reason why the conventional excitation-probe method can hardly discriminate the TPA and SRS signals. However, if the quantum mechanical nature of the optical modes is harnessed, the intensity change due to TPA and SRS can be distinguished.

In this paper, we propose a method to suppress the contribution of TPA to the excitation-probe signal by controlling the quantum states of the excitation and probe pulses. We have applied the proposed method to simulate the excitation-probe signal of a model material system and demonstrate herein that the proposed method can suppress the TPA signal and select the SRS signal specifically.

## 2. Theory

Fig. 1a shows the proposed measurement setup. Here the photon pairs can be produced in pulsed mode by means of spontaneous parametric down conversion (SPDC). A type-I nonlinear crystal is pumped by a Gaussian pulse with temporal duration  $T_1$  and central frequency  $\omega_p$ . The pulsed photon pairs can be described by a non-separable wave function  $|\Psi\rangle$  [12]:

$$|\Psi\rangle = \sum_{i,j} \phi_{ij} b_{1i}^\dagger b_{2j}^\dagger |0\rangle, \quad (1)$$

$$\phi_{ij} = C \exp[-T_1^2 [(\omega_p - \omega_{1i} - \omega_{2j})^2] \text{sinc}[T_2(\omega_{2j} - \omega_{1i})]] \quad (2)$$

where  $T_2$  is the entanglement time, defined by the difference between the inverse group velocities of the two photons.  $T_2$  can be controlled by changing the thickness of the SPDC crystal. Fock state  $b_{1i}^\dagger b_{2j}^\dagger |0\rangle$  has one photon in each mode  $k_1$  and  $k_2$ .  $C$  is proportional to the nonlinearity of the SPDC crystal and the pump electric field amplitude  $E_{\text{ex}}$  [13].

Inspired by the work of Roslyak *et al.*, we included an interferometer to control the quantum states of pulsed photon pairs [9]. The two photon modes  $(k_1, \omega_1)$  and  $(k_2, \omega_2)$  produced in the nonlinear crystal are directed into the input port of the broadband 50/50 beam splitter, which mixes the photon fields. The photons leaving the beam splitter can be described by  $a_1$  for the excitation photon field and  $a_2$  for the probe photon field [14]:

$$a_1 = \frac{1}{\sqrt{2}}(-b_1 + i b_2), \quad a_2 = \frac{1}{\sqrt{2}}(i b_1 - b_2). \quad (3)$$

We assumed that the excitation-probe signal is composed of eight pathway contributions [3,9]. When the proposed setup is used, the following six photon correlation functions among the eight functions are all equal to zero:

$$\begin{aligned} \langle a_1^\dagger a_2^\dagger a_2 a_1 \rangle &= \langle a_1^\dagger a_2^\dagger a_1 a_2 \rangle = \langle a_2^\dagger a_1^\dagger a_2 a_1 \rangle = \langle a_2^\dagger a_1^\dagger a_1 a_2 \rangle = \langle a_1^\dagger a_1 a_2^\dagger a_2 \rangle \\ &= \langle a_2^\dagger a_2 a_1^\dagger a_1 \rangle = 0. \end{aligned} \quad (4)$$

Calculations of these functions are given in Appendix A. Nonzero contributions thus arise only from the other two pathways;  $\langle a_2^\dagger a_1 a_1^\dagger a_2 \rangle$  of the (vi) pathway and  $\langle a_1^\dagger a_2 a_2^\dagger a_1 \rangle$  of the (viii) pathway.

We considered crystalline LaMnO<sub>3</sub> as the model material system. To mimic one lattice layer of the orbital- and spin-ordered LaMnO<sub>3</sub> crystal, we built a Hamiltonian for an ideal Mn cluster composed of four Mn<sup>3+</sup> ions. Details of the model material system and the

Hamiltonian can be found in Ref. [15].

Fig. 1b schematically illustrates the structure of the material system's energy eigenstates.  $|g\rangle$  represents a set of eigenstates, i.e.  $\{|g_1\rangle, |g_2\rangle, \dots; |g_1\rangle$  is the ground state. The energy difference between  $|g_n\rangle$  and  $|g_{n+1}\rangle$  arises from the phonon-orbital coupling energy difference for the different octahedral distortion and orbital ordering configuration. The second set,  $|e\rangle = \{|e_1\rangle, |e_2\rangle, \dots\}$ , represents the set of photoexcited eigenstates. The excited state corresponds to one hole and one double-occupied state. The energy difference between  $|e_n\rangle$  and  $|e_{n+1}\rangle$  arises from phonon-orbital coupling between the sites, similar as in  $\{|g_n\rangle\}$ . The energy difference between  $|g_n\rangle$  and  $|e_n\rangle$  arises mainly from Coulomb energy ( $U$ ), since  $U$  is about 10 times the phonon-orbital coupling energy. The third set of higher-energy ( $\sim 2U$ ) photoexcited states,  $|f\rangle$  (not shown in Fig. 1a), is also considered in the interaction process. The values of  $U$ ,  $J$ ,  $Q_3$ ,  $q$ , and  $\omega_{ph}$  used in the calculations were  $5t$ ,  $0.06t$ ,  $0.27t$ ,  $0.07t$ , and  $0.2t$ , respectively.  $t$  is the hopping integral parameter representing the kinetic energy gain of the Mn ion electrons [14].

In the proposed excitation-probe setup, the probe signal is determined solely by the (vi) and (viii) pathways; loop diagrams for these pathways are given in Fig. 1c. In the (vi) pathway, the system evolves from the ground state  $(|g\rangle)$  to an excited state  $(|e\rangle)$  by absorbing a photon, then to a low-energy state  $(|g'\rangle)$  by emitting a photon. Then it assumes another excited state  $(|e'\rangle)$  by absorbing a photon, then finally returns to the ground state  $(|g\rangle)$  by emitting a photon. In the (viii) pathway, the system undergoes evolution from the ground state  $(|g\rangle)$  to an excited state  $(|e\rangle)$  by absorbing a photon, then to a low-energy state  $(|g'\rangle)$  by emitting a photon; then, the same process is repeated once in the bra-vectors.

The frequency-resolved signal,  $S(\omega_1, \omega_2)$ , is given by the following equation [3]:

$$S(\omega_1, \omega_2) \sim \text{Im}[\chi^{(vi)}(\omega_1, \omega_2)] \langle a_2^\dagger a_1 a_1^\dagger a_2 \rangle + \text{Im}[\chi^{(viii)}(\omega_1, \omega_2)] \langle a_1^\dagger a_2 a_2^\dagger a_1 \rangle. \quad (5)$$

The third-order material susceptibility functions are as follows:

$$\chi^{(vi)}(\omega_1, \omega_2) = \frac{-1}{3!} \sum_e \sum_{g'} \sum_{g''} \mu_{g_1 e}^\beta \mu_{e g'}^\alpha \mu_{g' g''}^\beta \mu_{g'' e}^\alpha \mu_{e g_1}^\beta g_{g' g_1}(\omega_2) g_{g' g_1}(\omega_2 - \omega_1) g_{e g_1}(\omega_2) \quad (6)$$

$$\chi^{(viii)}(\omega_1, \omega_2) = \frac{-1}{3!} \sum_e \sum_{g'} \sum_{g''} \mu_{g_1 e}^\alpha \mu_{e g'}^\beta \mu_{g' g''}^\alpha \mu_{g'' e}^\beta g_{g' g_1}^*(\omega_1) g_{e g_1}^*(\omega_1 - \omega_2) g_{e g_1}^*(\omega_1) \quad (7)$$

here,  $\mu_{eg}^{\alpha,\beta}$  is the dipole matrix element between the two energy eigenstates  $|e\rangle$  and  $|g\rangle$  of the full Hamiltonian (H), namely,  $\langle e | \vec{r} | g \rangle$ ;  $\vec{r}$

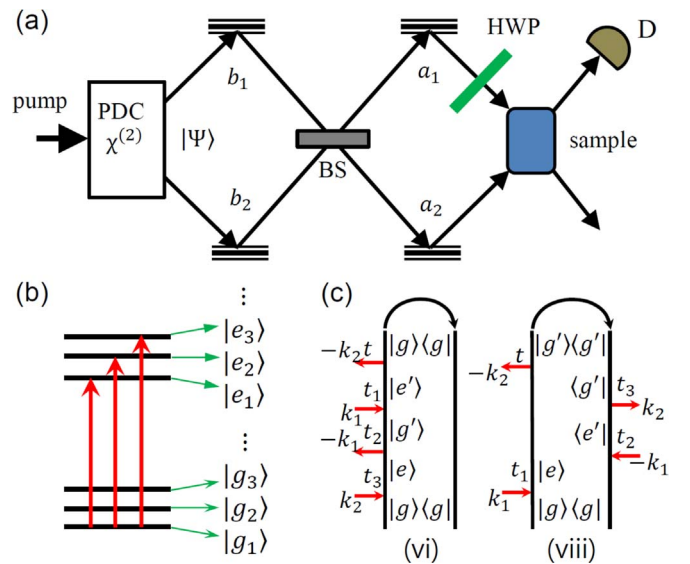


Fig. 1. (a) Proposed excitation-probe setup, (b) schematic structure of energy eigenstates of the model material system, and (c) closed-time path-loop diagrams for (vi) and (viii) pathways.

Download English Version:

<https://daneshyari.com/en/article/7926977>

Download Persian Version:

<https://daneshyari.com/article/7926977>

[Daneshyari.com](https://daneshyari.com)